Molecular Cell, Volume *81*

Supplemental information

Proteome dynamics at broken replication forks reveal a distinct ATM-directed repair response suppressing DNA double-strand break ubiquitination

Kyosuke Nakamura, Georg Kustatscher, Constance Alabert, Martina Hödl, Ignasi Forne, Moritz Völker-Albert, Shankha Satpathy, Tracey E. Beyer, Niels Mailand, Chunaram Choudhary, Axel Imhof, Juri Rappsilber, and Anja Groth

Figure S1

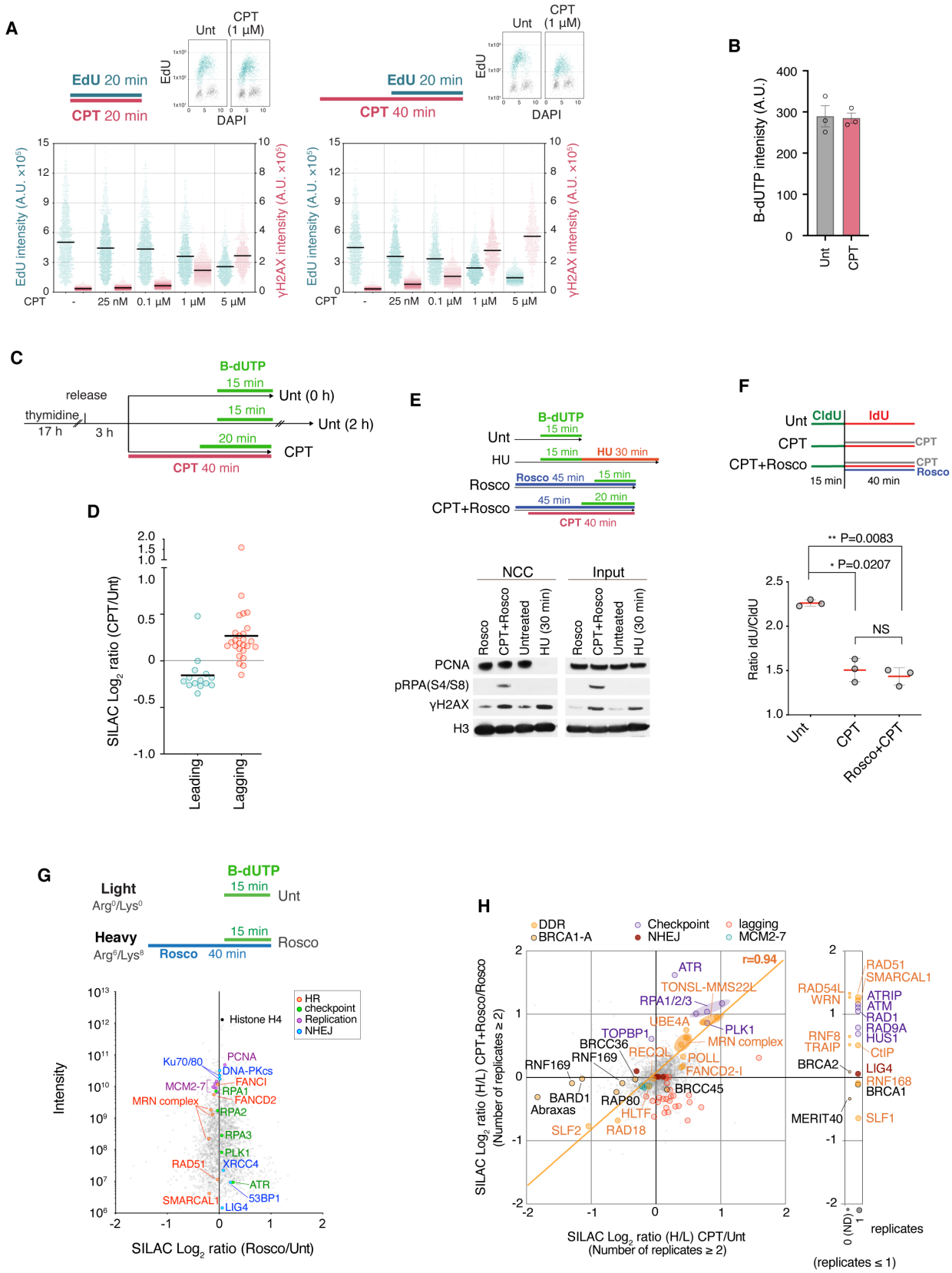
A
EdU 20 min
CPT 20 min
Unt
CPT (1 μM)
EdU
DAPI
EdU 20 min
CPT 40 min
EdU intensity (A.U. ×10⁵)
γH2AX intensity (A.U. ×10⁵)
CPT
25 nM
0.1 μM
1 μM
5 μM
B
B-dUTP intensity (A.U.)
Unt
CPT
C
B-dUTP
15 min
release
thymidine
17 h
3 h
Unt (0 h)
Unt (2 h)
20 min
CPT
CPT 40 min
D
SILAC Log2 ratio (CPT/Unt)
Leading
Lagging
E
B-dUTP
Unt
HU
HU 30 min
Rosco
Rosco 45 min
CPT+Rosco
45 min
CPT 40 min
NCC
Input
Rosco
CPT+Rosco
Untreated
HU (30 min)
Untteated
PCNA
pRPA(S4/S8)
γH2AX
H3
F
Unt
CldU
IdU
CPT
CPT+Rosco
Rosco
15 min
40 min
** P=0.0083
* P=0.0207
NS
Ratio IdU/CldU
Unt
CPT
Rosco+CPT
G
Light
Arg0/Lys0
Heavy
Arg6/Lys8
B-dUTP
15 min
Unt
Rosco
Rosco 40 min
HR
checkpoint
Replication
NHEJ
Histone H4
PCNA
Ku70/80
DNA-PKcs
FANCI
MCM2-7
RPA1
FANCD2
MRN complex
RPA2
RPA3
PLK1
XRCC4
RAD51
ATR
53BP1
SMARCAL1
LIG4
Intensity
SILAC Log2 ratio (Rosco/Unt)
H
DDR
BRCA1-A
Checkpoint
NHEJ
lagging
MCM2-7
r=0.94
ATR
TONSL-MMS22L
RPA1/2/3
UBE4A
PLK1
MRN complex
TOPBP1
BRCC36
RECQL
POLL
FANCD2-I
RNF169
BRCC45
BARD1
Abraxas
RAP80
HLTF
SLF2
RAD18
SILAC Log2 ratio (H/L) CPT+Rosco/Rosco
(Number of replicates ≥ 2)
SILAC Log2 ratio (H/L) CPT/Unt
(Number of replicates ≥ 2)
RAD51
SMARCAL1
RAD54L
WRN
ATRIP
ATM
RAD1
RAD9A
HUS1
RNF8
TRAIP
CtIP
BRCA2
LIG4
RNF168
BRCA1
MERIT40
SLF1
0 (ND)
1
replicates
(replicates ≤ 1)

Figure S1. Proteomic analysis of broken replication forks, Related to Figure 1

(A) High-content microscopy of CPT-induced γH2AX and new DNA synthesis. Top, experimental design for optimization of CPT treatment for NCC, aiming to induce high levels of DNA damage while maintaining DNA synthesis. EdU positive cells were defined by gating on mean EdU intensity and DAPI (insets). Bottom, scatter plots show total intensity of EdU (blue) and γH2AX (red) in EdU positive cells. **(B)** Analysis of biotin-dUTP (B-dUTP) incorporation under conditions used for SILAC-NCC-MS (CPT/Unt) analysis of CPT-treated cells as detailed in in Figure 1A. HeLa-S3 cells were labelled 20 min (CPT) or 15 min (Unt) with B-dUTP in the presence or absence of CPT treatment (see Figure 1A) before pre-extraction and immunofluorescence analysis. The mean intensity in B-dUTP positive cells is shown with SEM, n=3. Individual data points are indicated by dots and correspond to the mean of >142 cells. **(C)** Experimental design for Figure 1B. **(D)** Enrichment of core replication factors. Leading and lagging strand associated proteins are separated as in Figure 1G. Black bars indicate mean. **(E)** Top, experimental design for NCC western blot analysis of CPT, HU, and roscovitine (Rosco) treated cells. Bottom, NCC pulldown analyzed by western blotting. **(F)** DNA fiber analysis of cells treated with CPT and Rosco. Mean ratio of IdU/CldU length are shown with SEM, n=3 independent experiments; from left P=0.0207, 0.0111, NS, not significant (P=0.2173), ratio paired two-sided t-test. Data points are indicated by dots and correspond to the mean of 50 CldU-IdU tracks from three independent experiments. **(G)** Top, experimental design for NCC-SILAC-MS analysis of cell treated with and without Rosco (Rosco/Untreated). Bottom, enrichment of DDR proteins, given as the mean of three independent experiments. **(H)** Correlation plot showing replication and DDR proteins identified in CPT+Rosco/Rosco and CPT/Unt NCC-SILAC-MS. The proteins identified in ≤ 1 replicates in CPT/Unt are shown on the right. Pearson correlation (r) of DDR proteins are shown.

Figure S2

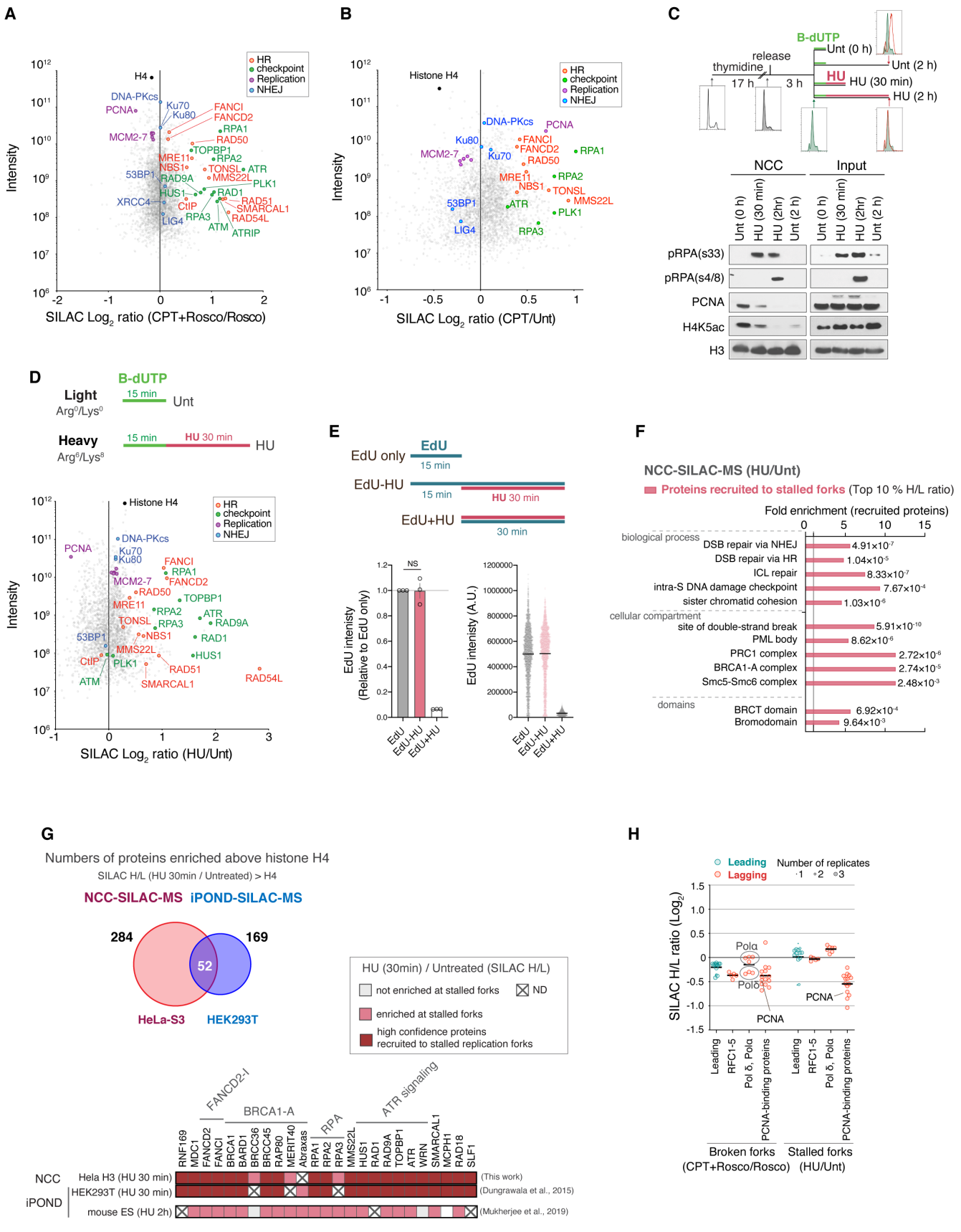
A
B
C
D
E
F
G
H
Intensity
SILAC Log2 ratio (CPT+Rosco/Rosco)
SILAC Log2 ratio (CPT/Unt)
SILAC Log2 ratio (HU/Unt)
HR
checkpoint
Replication
NHEJ
Histone H4
B-dUTP
release
thymidine
17 h
3 h
Unt (0 h)
Unt (2 h)
HU
HU (30 min)
HU (2 hr)
NCC
Input
pRPA(s33)
pRPA(s4/8)
PCNA
H4K5ac
H3
Light
Arg0/Lys0
Heavy
Arg6/Lys8
15 min
Unt
HU 30 min
EdU only
EdU
EdU-HU
EdU+HU
30 min
EdU intensity (Relative to EdU only)
EdU intensity (A.U.)
NS
NCC-SILAC-MS (HU/Unt)
Proteins recruited to stalled forks (Top 10 % H/L ratio)
Fold enrichment (recruited proteins)
biological process
DSB repair via NHEJ
DSB repair via HR
ICL repair
intra-S DNA damage checkpoint
sister chromatid cohesion
cellular compartment
site of double-strand break
PML body
PRC1 complex
BRCA1-A complex
Smc5-Smc6 complex
domains
BRCT domain
Bromodomain
Numbers of proteins enriched above histone H4
SILAC H/L (HU 30min / Untreated) > H4
NCC-SILAC-MS
iPOND-SILAC-MS
284
169
52
HeLa-S3
HEK293T
HU (30min) / Untreated (SILAC H/L)
not enriched at stalled forks
ND
enriched at stalled forks
high confidence proteins recruited to stalled replication forks
FANCD2-I
BRCA1-A
RPA
ATR signaling
NCC
iPOND
Hela H3 (HU 30 min)
HEK293T (HU 30 min)
mouse ES (HU 2h)
(This work)
(Dungrawala et al., 2015)
(Mukherjee et al., 2019)
Leading
Lagging
Number of replicates
SILAC H/L ratio (Log2)
Pola
Polδ
PCNA
RFC1-5
Pol δ, Pola
PCNA-binding proteins
Broken forks
(CPT+Rosco/Rosco)
Stalled forks
(HU/Unt)

Figure S2. Protein composition of broken and stalled replication forks, Related to Figure 2

(A), (B) Enrichment of replication and DDR proteins, considering only high confidence factors identified in ≥2 NCC-SILAC-MS experiments of (CPT+Rosco/Rosco) (**A**) and (CPT/Unt) (**B**). Enrichments are given as the mean log_2 SILAC ratios of three independent experiments. **(C)** Top, experimental design for NCC western blot analysis of stalled replication forks. Cells were labelled 15 min with B-dUTP and treated with 3 mM HU as indicated. Cell cycle profiles are shown to illustrate that HU blocks DNA replication. Bottom, NCC pulldown analyzed by western blotting. **(D)** Top, experimental design for NCC-SILAC-MS analysis of HU stalled replication forks (HU/Unt). Bottom, enrichment of replication and DDR proteins as in (A). (**E**) Top, experimental design for EdU incorporation upon HU treatment. Bottom left, high-content microscopy of EdU. The mean intensity in EdU positive cells is shown with SEM. n=3 independent experiments. NS, not significant by ratio paired two-sided t-test. Bottom right, one representative experiment is shown. The bars indicate mean. From left n=2052, 2305, and 1909. **(F)** GO analysis of the proteins recruited to stalled forks (top 10 % enriched based on H/L ratio). **(G)** Top, overlap between NCC-SILAC-MS and iPOND-SILAC-MS (Dungrawala et al., 2015) analyses of HU stalled replication forks. The number of proteins enriched at stalled replication forks above histone H4 (Log2 HU/Unt SILAC ratio > H4) are shown. Given the technical differences, SILAC ratios are not directly comparable. We thus use histone H4, robustly identified by both methods, to set a threshold for protein enrichment at stalled replication forks. 52 factors are identified by NCC and iPOND in cells treated 30 min with HU (see Table S2). Bottom, high confidence DDR proteins recruited to stalled replication forks (identified by both NCC and iPOND). Enrichment in iPOND-SILAC-MS in mouse ES cells (Mukherjee et al., 2019) is included for comparison. **(H)** Enrichment of leading and lagging strand associated proteins at broken (CPT+Rosco/Rosco) and stalled (HU/Unt) replication forks. Symbol size indicates number of replicates in which a protein was identified.

Figure S3

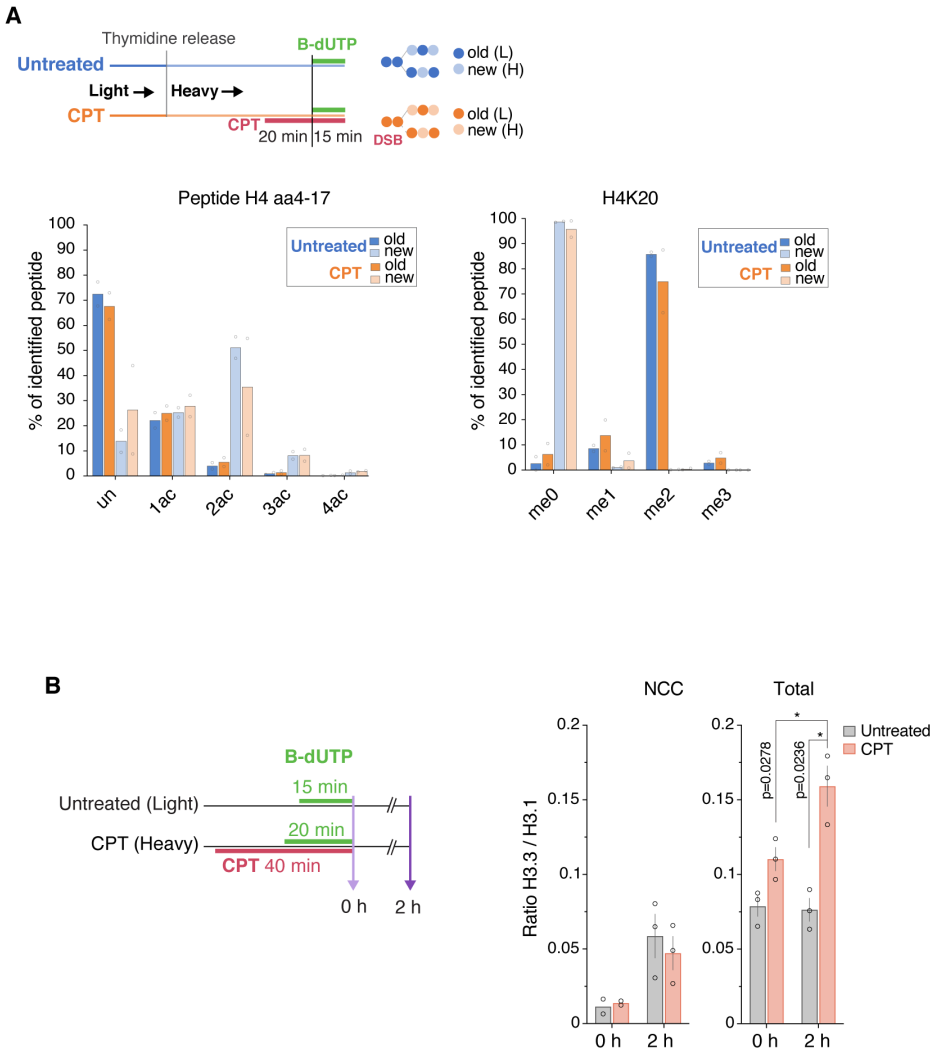

Figure S3. Histone PTM analysis, Related to Figure 3

(A) Top, design of NCC-pulse SILAC-MS experiment to track acetylation (bottom left) and methylation (bottom right) on new (light color) and old (dark color) histone H4 in CPT (orange) and untreated (blue) cells. Different modification states are shown as the percentage total peptide identified. The H4 amino acid 4–17 (aa4–17) peptide contains four potential acetylation sites (K5, K8, K12, and K16). (Un) Unmodified; (ac) acetylated; (ac2) diacetylated; (ac3) triacetylated; (ac4) quadriacetylated. me0, unmethylated; me1, mono-methylated; me2, di-methylated; me3, tri-methylated. Bars show the mean of two independent experiments (n=2), with individual measurements indicated by dots. **(B)** Left, experimental design for analysis of histones SILAC-NCC-MS. Right, the ratio of histone H3.3/H3.1 are shown. NCC, NCC pulldown of nascent (0 h) and mature (2 h) chromatin (B-dUTP labelled chromatin); Total, bulk chromatin. The mean is shown with SEM. n=3 independent experiments. *, significant by ratio paired two-sided t-test.

Figure S4

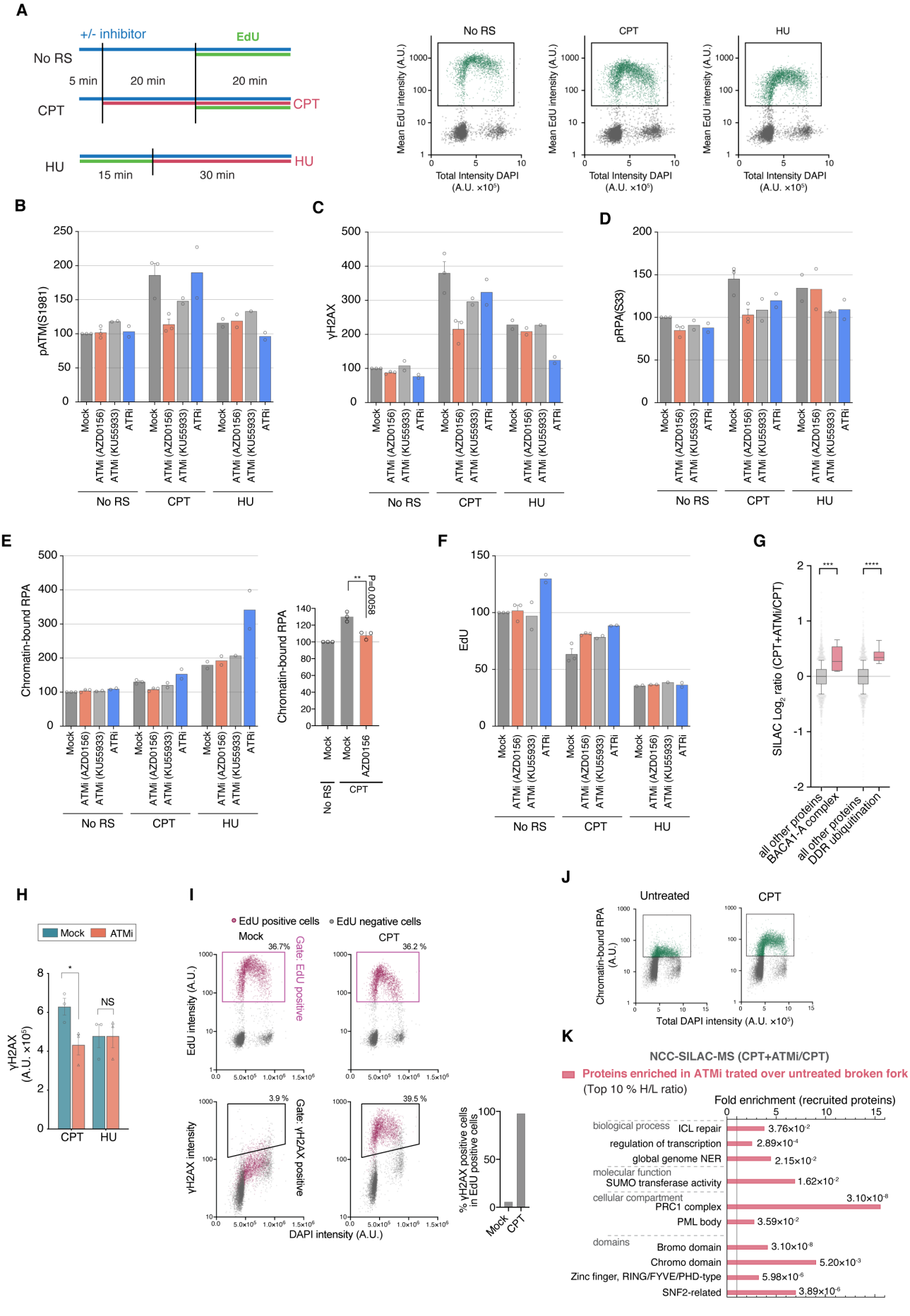
A
+/- inhibitor
EdU
No RS
5 min
20 min
20 min
CPT
CPT
HU
HU
15 min
30 min
No RS
CPT
HU
Mean EdU intensity (A.U.)
Total Intensity DAPI (A.U. ×10⁵)
B
pATM(S1981)
C
γH2AX
D
pRPA(S33)
Mock
ATMi (AZD0156)
ATMi (KU55933)
ATRi
No RS
CPT
HU
E
Chromatin-bound RPA
P=0.0058
F
EdU
G
SILAC Log2 ratio (CPT+ATMi/CPT)
all other proteins
BACA1-A complex
all other proteins
DDR ubiquitination
H
Mock
ATMi
γH2AX (A.U. ×10⁵)
NS
I
EdU positive cells
EdU negative cells
Gate: EdU positive
36.7%
36.2 %
Gate: γH2AX positive
3.9 %
39.5 %
DAPI intensity (A.U.)
% γH2AX positive cells in EdU positive cells
J
Untreated
CPT
Chromatin-bound RPA (A.U.)
Total DAPI intensity (A.U. ×10⁵)
K
NCC-SILAC-MS (CPT+ATMi/CPT)
Proteins enriched in ATMi trated over untreated broken fork
(Top 10 % H/L ratio)
Fold enrichment (recruited proteins)
biological process
ICL repair
3.76×10-2
regulation of transcription
2.89×10-4
global genome NER
2.15×10-2
molecular function
SUMO transferase activity
1.62×10-2
cellular compartment
PRC1 complex
3.10×10-8
PML body
3.59×10-2
domains
Bromo domain
3.10×10-8
Chromo domain
5.20×10-3
Zinc finger, RING/FYVE/PHD-type
5.98×10-6
SNF2-related
3.89×10-6

Figure S4. Dissecting ATM function at broken replication forks, Related to Figure 4

(A) Left, experimental design for analyzing ATM dependent responses to CPT and HU. Right, gating strategy to identify S phase cells (EdU positive) is shown. RS, replication stress. **(B)-(F)** High-content microscopy of pATM-S1981 (**B**), γH2AX (**C**), pRPA-S33 (**D**), RPA (**E**) and EdU (**F**) in EdU positive cells is shown relative to mock/no RS. ATMi, 10 μM KU-55933 or 250 nM AZD0156. ATRi, 300 nM AZ20. U-2-OS cells were treated with CPT according to the scheme developed for NCC-SILAC-MS shown in (A). (E, right panel) **, P=0.0058 by ratio paired two-sided t-test. **(G)** Comparison of SILAC Log2 ratios between the indicated protein categories (BRCA1-A complex, factors promoting DDR ubiquitination) and all other proteins. ***, P<0.001; ****, P<0.0001 by Mann-Whitney U test. **(H)** High-content microscopy of γH2AX accumulation upon CPT or HU treatment, as control for Figure 4D, E. U-2-OS cells were exposed to 1 μM CPT or 3 mM HU for 1 h. The cells were pre-extracted and analyzed by immunofluorescence. ATMi (AZD0156) was added 5 min before treatment with CPT or HU. The intensity in γH2AX positive cells is shown with SEM. n=3 independent experiments. *, P=0.0312; NS, not significant by ratio paired two-sided t-test. Data points are indicated by dots and correspond to the mean of >3937 cells. (**I**) Gating strategy for γH2AX positive cells. CPT induced γH2AX positive cells are highly overlapped with EdU positive (S phase) cells. **(J)** Gating strategy for RPA positive cells quantified in Figure 4E. **(K)** GO analysis of the proteins recruited to CPT treated forks upon inhibition of ATM signaling (top 10 % enriched based on H/L ratio (CPT+ATMi/CPT)).

Figure S5

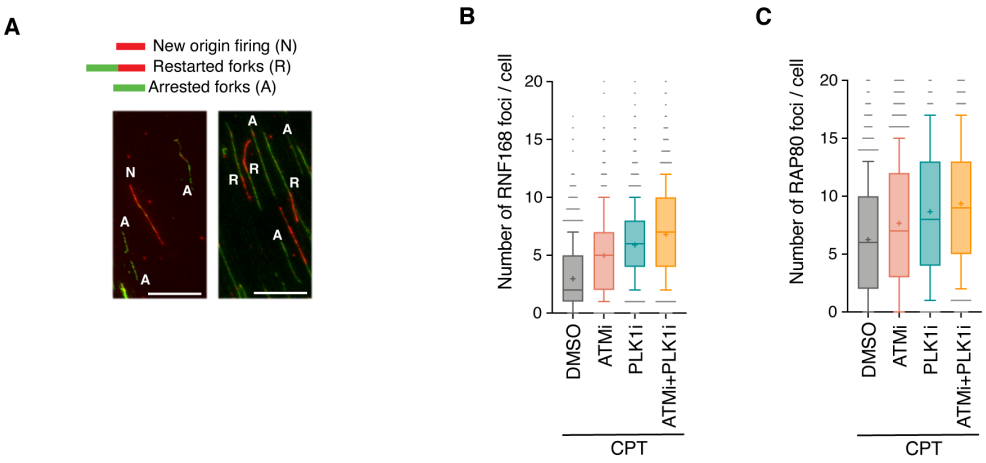

Figure S5. Regulation of H2A ubiquitination by ATM and PLK1 at broken replication forks, Related to Figure 5

(A) Representative images to illustrate identification of new origins, restarted forks and arrested forks in Figure 5A. Cells were incubated CIdU (green) followed by IdU (red). Scale bar, 15 μm. (**B, C**) Representative experiments from Figure 5B, C. Mean is shown (+) with whiskers indicate 10-90 percentile; From left in (B), n = 2805, 1960, 2518, and 2254 cells. From left in (C), n = 2117, 1879, 2052, and 1894 cells.

Figure S6

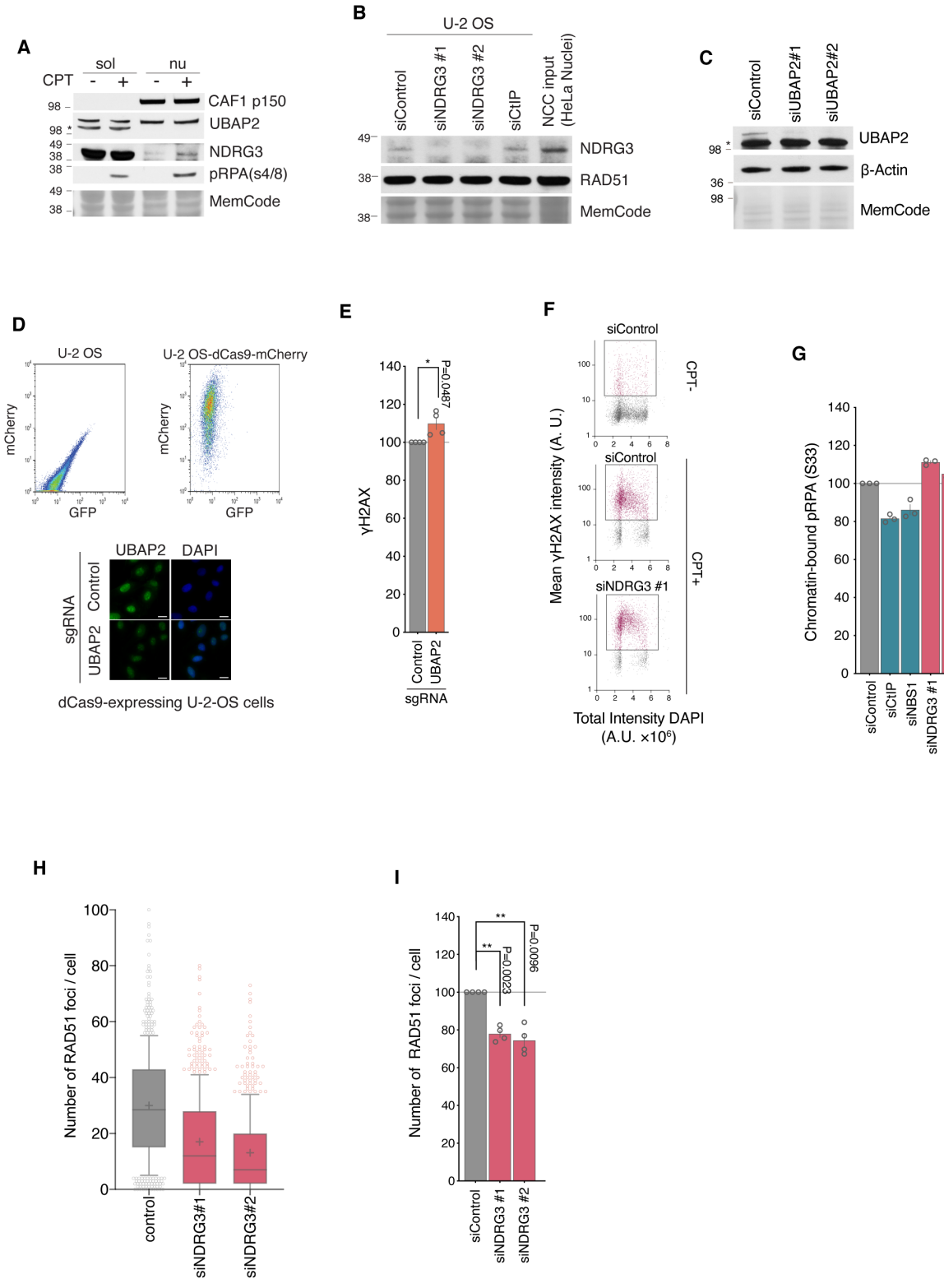
A
sol
nu
CPT - + - +
CAF1 p150
UBAP2
NDRG3
pRPA(s4/8)
MemCode
B
U-2 OS
siControl
siNDRG3 #1
siNDRG3 #2
siCtIP
NCC input (HeLa Nuclei)
NDRG3
RAD51
MemCode
C
siControl
siUBAP2#1
siUBAP2#2
UBAP2
β-Actin
MemCode
D
U-2 OS
U-2 OS-dCas9-mCherry
mCherry
GFP
UBAP2
DAPI
sgRNA
Control
UBAP2
dCas9-expressing U-2-OS cells
E
γH2AX
P=0.0487
Control
UBAP2
sgRNA
F
siControl
siNDRG3 #1
CPT-
CPT+
Mean γH2AX intensity (A. U.)
Total Intensity DAPI (A.U. ×10⁶)
G
Chromatin-bound pRPA (S33)
siControl
siCtIP
siNBS1
siNDRG3 #1
siNDRG3 #2
H
Number of RAD51 foci / cell
control
siNDRG3#1
siNDRG3#2
I
Number of RAD51 foci / cell
P=0.0096
P=0.0023
siControl
siNDRG3 #1
siNDRG3 #2

Figure S6. NDRG3 is required for RAD51 regulation upon CPT, Related to Figure 6

(A) Western blot analysis of NDRG3 and UBAP2 localization. HeLa S3 cells were treated as indicated (CPT, 1 μM for 1 h) and nuclear (nu) and cytosolic (sol) extract were harvested for western blotting as described (Jasencakova et al., 2010). CAF1 p150 was used as a fractionation control. One representative experiment is shown of three biological replicates. Asterisk indicates non-specific bands. **(B)** Western blot analysis of NDRG3 and RAD51 in siRNA transfected cells. **(C)** Western blot analysis of UBAP2 in siRNA transfected U-2-OS cells. Asterisk indicates non-specific bands. (**D**)Top, flow cytometry analysis of dCAS9-mCherry expression. Bottom, validation of UBAP2-targeted sgRNA by immunofluorescence. Pre-extraction was performed before immunofluorescence analysis. Scale bar, 10 μm. (**E**) High-content microscopy of γH2AX. The cells were exposed to 1 μM CPT for 1 h before pre-extraction and immunofluorescence analysis. Mean intensity in γH2AX positive cells relative to control sgRNA is shown. Error bars indicate SEM., n=4. *, significant by ratio paired two-sided t-test. **(F**, **G)** High-content microscopy of siRNA transfected U-2-OS cells treated with 1 μM CPT for 1 h prior to pre-extraction and analysis by immunofluorescence. (**F**) Gating strategy to identify γH2AX positive cells. (**G**) Analysis of phospho-RPA(Ser33) in γH2AX positive cells. Bars show mean with SEM, n=3. Data points are indicated by dots and correspond to the mean of >1391 cells. (**H**) Representative experiment related to Figure 6F. Mean is shown (+) with whiskers indicate 10-90 percentile; from left, n = 608, 616, 563. (**I**) High-content microscopy of RAD51 foci. siRNA transfected U-2-OS cells treated with 3 mM HU for 2 h prior to pre-extraction and analysis by immunofluorescence. Bar-diagram showing the number of RAD51 foci in γH2AX positive cells relative to control siRNA treatment. Mean with error bars showing SEM, n=4. Data points are indicated by dots and correspond to the mean of >3187 cells.

Figure S7

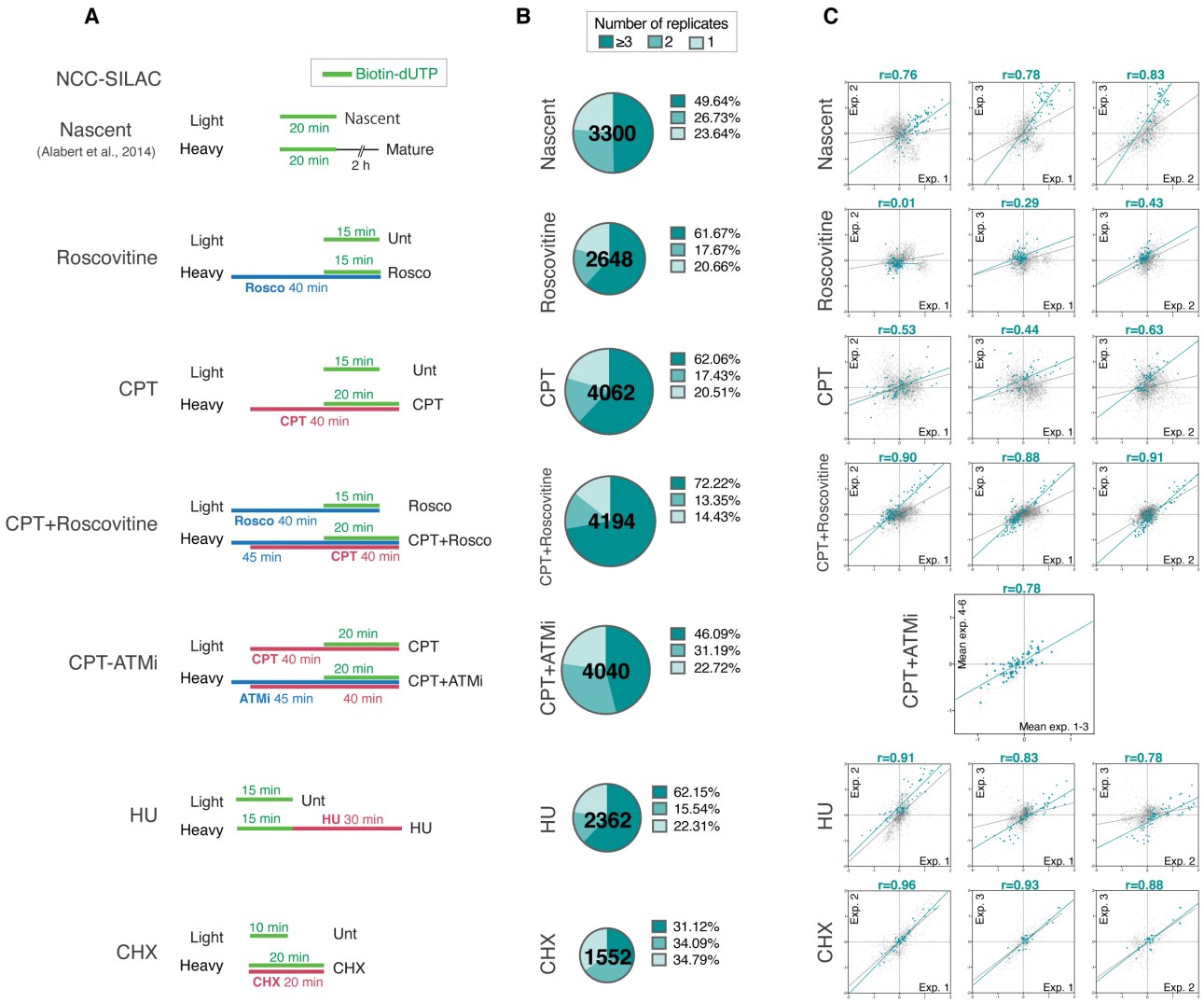

Figure S7. NCC-SILAC-MS data set resource, Related to Figure 1-6

(A) Experimental design for NCC-SILAC-MS experiments. Published Nascent/Mature data (Alabert et al., 2014) were reprocessed and normalized similar to the other data sets for comparison. **(B)** Number of identified proteins in NCC-SILAC-MS experiments across all replicates, considering only SILAC ratios detected by 2 or more ratio counts. **(C)** Scatter plots comparing Log2 SILAC ratios between replicates. The Pearson correlation of replication and DDR proteins (green) and for all identified proteins (grey) is shown, illustrating reproducibility.